Title
Third-Generation Synchrotron Light Source

Author
Schlachter, Alfred S.

Publication Date
1993-09-01

LBL-34749
UC-406

Lawrence Berkeley Laboratory
UNIVERSITY OF CALIFORNIA

Accelerator & Fusion
Research Division

Presented at the NATO Advanced Study Institute,
Maratea, Italy, June 28–July 10, 1992,
and to be published in the Proceedings

Third-Generation Synchrotron Light Sources

A.S. Schlachter

September 1993

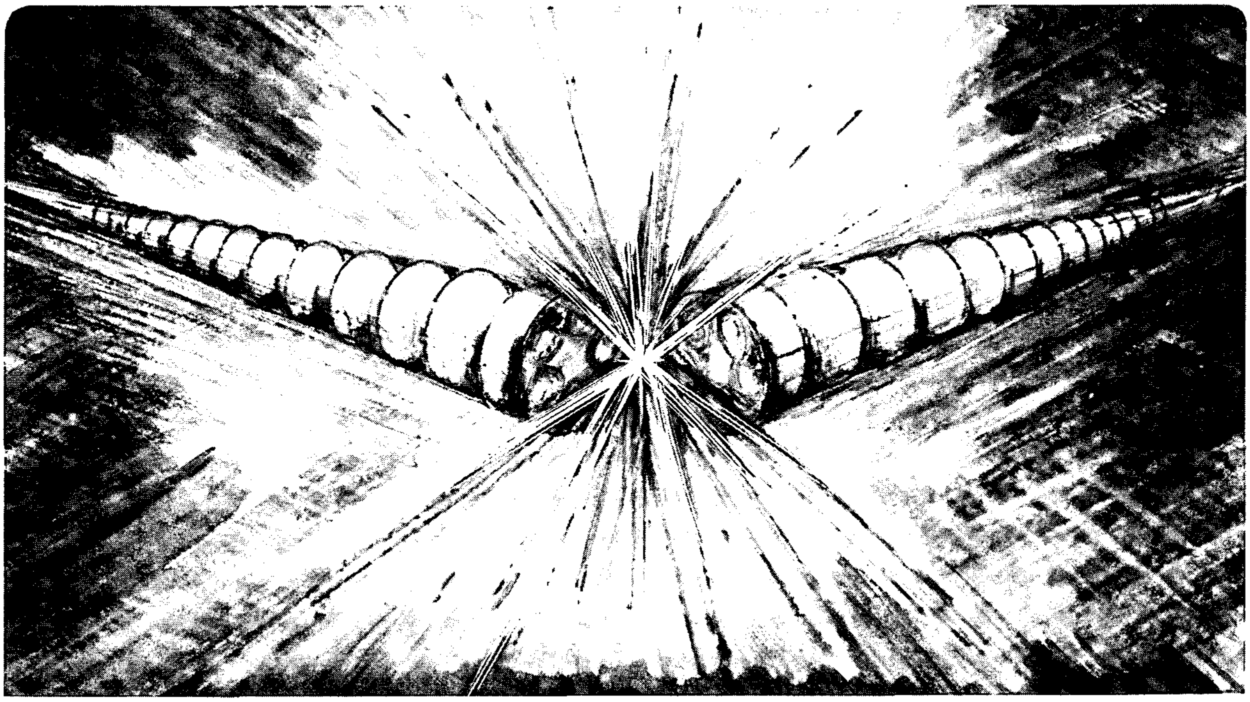

Prepared for the U.S. Department of Energy under Contract Number DE-AC03-76SF00098

DISCLAIMER

This document was prepared as an account of work sponsored by the United States Government. Neither the United States Government nor any agency thereof, nor The Regents of the University of California, nor any of their employees, makes any warranty, express or implied, or assumes any legal liability or responsibility for the accuracy, completeness, or usefulness of any information, apparatus, product, or process disclosed, or represents that its use would not infringe privately owned rights. Reference herein to any specific commercial product, process, or service by its trade name, trademark, manufacturer, or otherwise, does not necessarily constitute or imply its endorsement, recommendation, or favoring by the United States Government or any agency thereof, or The Regents of the University of California. The views and opinions of authors expressed herein do not necessarily state or reflect those of the United States Government or any agency thereof or The Regents of the University of California and shall not be used for advertising or product endorsement purposes.

This report has been reproduced directly from the best available copy.

Lawrence Berkeley Laboratory is an equal opportunity employer.

DISCLAIMER

LBL-34749
UC-406

Third-Generation Synchrotron Light Sources

A.S. Schlachter

To be published in the Proceedings of the
NATO Advanced Study Institute

New Directions in Research with Third-Generation
Soft X-Ray Synchrotron Radiation Sources

held in Maratea, Italy
June 28–July 10, 1992

Edited by:

A.S. Schlachter
Advanced Light Source
Lawrence Berkeley Laboratory
University of California
Berkeley, California 94720 USA

and

F.J. Wuilleumier
Laboratoire de Spectroscopie
Atomique et Ionique
Université Paris Sud
Orsay, France

This work was supported by the Director, Office of Energy Research, Office of Basic Energy Sciences, Materials Sciences Division, of the U.S. Department of Energy under Contract No. DE-AC03-76SF00098.

THIRD-GENERATION SYNCHROTRON LIGHT SOURCES

A.S. SCHLACHTER
Lawrence Berkeley Laboratory
University of California
Berkeley, CA 94720 USA

ABSTRACT. X rays are a powerful probe of matter because they interact with electrons in atoms, molecules, and solids. They are commonly produced by relativistic electrons or positrons stored in a synchrotron. Recent advances in technology are leading to the development of a new third generation of synchrotron radiation sources that produce vacuum-ultraviolet and x-ray beams of unprecedented brightness. These new sources are characterized by a very low electron-beam emittance and by long straight sections to accommodate permanent-magnet undulators and wigglers. Several new low-energy light sources, including the Advanced Light Source, presently under construction at the Lawrence Berkeley Laboratory, and ELETTRA, presently being constructed in Trieste, will deliver the world's brightest synchrotron radiation in the VUV and soft x-ray regions of the spectrum. Applications include atomic and molecular physics and chemistry, surface and materials science, microscopy, and life sciences.

1. Introduction

Light is one of the most important tools of science. It is the key to viewing the universe—from distant galaxies to cells, molecules, and even atoms. Light has a dual nature, behaving both as a stream of massless particles (photons) and as electromagnetic waves moving through space.

Visible light, which enables us to see the everyday objects around us, is easily generated and easy to detect. The sun, electric lamps, and fire produce it. We can see visible light with our eyes and detect it with photographic film; however, it constitutes only a tiny fraction of the full electromagnetic spectrum (see Fig. 1).

The remainder of the spectrum consists of light with wavelengths longer or shorter than those of visible light. On the longer side are radio waves, microwaves, and infrared radiation. Shorter-wavelength light includes ultraviolet, x rays, and gamma rays. These regions of the spectrum are invisible to the eye and must be detected by special means. Each region has a characteristic range of wavelengths and photon energies that determine the degree to which the light will penetrate and interact with matter. Light sources relevant to this institute produce radiation in the vacuum-ultraviolet and soft x-ray regions of the spectrum. This light is useful for several reasons:

- It can penetrate materials opaque to visible light (see Fig. 2).
- It has the right wavelengths—from about 10^{-7} to 10^{-10} meter—for exploring the atomic structure of solids, molecules, and important biological structures. The sizes of atoms, molecules, and proteins as well as the lengths of chemical bonds and the minimum distances between atomic planes in crystals are in this range (see Fig. 3). High-resolution x-ray microscopy is one technique used for such exploration. The combination of wavelengths shorter than visible light and the possibility of obtaining contrast through the

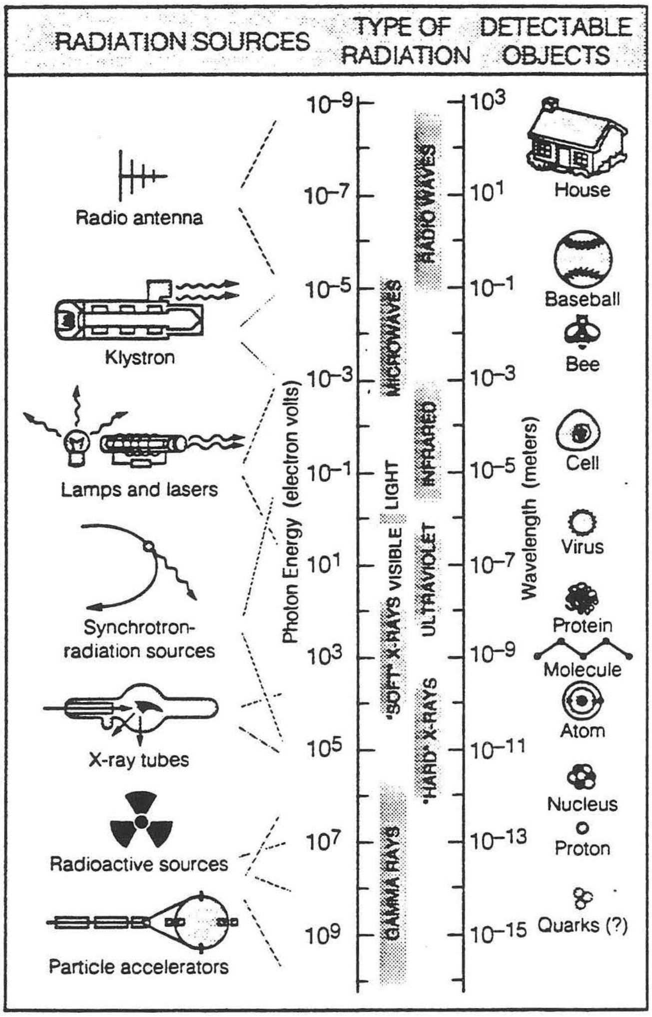

Figure 1. The electromagnetic spectrum covers a wide range of wavelengths and photon energies. (From "Synchrotron Radiation," by H. Winick. Copyright © 1987 by Scientific American, Inc. All rights reserved.)

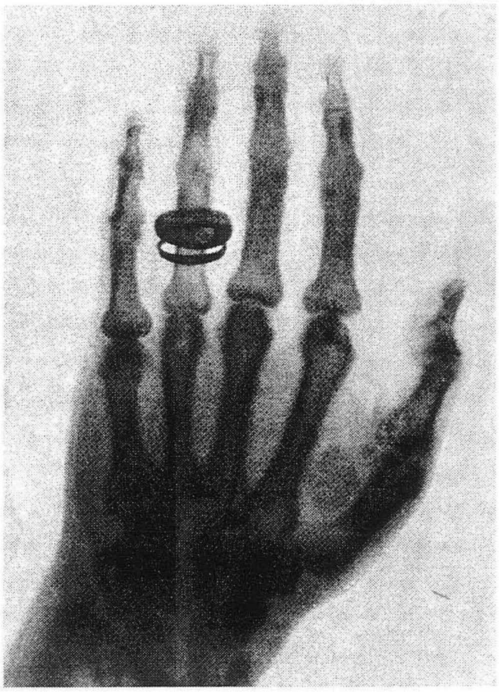

Figure 2. This image was made in 1896 by Wilhelm C. Roentgen, who discovered x rays and put them to practical use. (From O. Glasser, Wilhelm *Conrad Roentgen, The Early History of the Roentgen Rays*, 1934.)

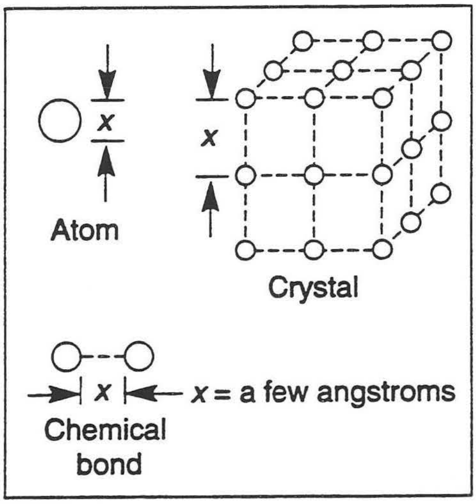

Figure 3. Atoms, chemical bonds, and the distances between atomic planes in crystals all measure a few angstroms—corresponding to the wavelengths of light in the x-ray energy range.

interaction of x rays with atoms in the material being examined makes this technique feasible (see Fig. 4).

- It has photon energies from about 10 to 10,000 electron volts. This energy range corresponds with the binding energy of many electrons in atoms, molecules, solids, and biological systems. Absorption of photons by an atom shows a large increase when the photon energy is sufficient to remove an electron from a given shell of that atom. The photon energies (or wavelengths) at which such increased absorption occurs—called absorption edges—are characteristic of the atom (see Fig. 5). Experiments using this principle can not only determine which atoms are present in the material under study but also can reveal information about the chemical state of the atoms (see Fig. 6).

2. Synchrotron Radiation

Whenever a charged particle such as an electron is accelerated or decelerated, it produces photons. At low velocities, electrons in a curved trajectory emit light of low intensity and low frequency in all directions; however, at relativistic speeds, the intensity, frequency, and collimation of the emitted light increase dramatically. Light generated by bending the path of relativistic electrons is called synchrotron radiation (see Fig. 7).

The natural emission angle for radiation emitted by a relativistic electron is $1/\gamma$, where γ is the ratio of the moving mass to the rest mass of the electron. In practical units, this is $1957E$ (where E is the electron energy in GeV). The value of γ is approximately 3000 for a 1.5-GeV electron; thus the natural angle for photons emitted at this energy is of the order of 0.3 milliradian.

The power P emitted by a relativistic electron is proportional to the fourth power of the electron energy E:

$$P = 2e^2c\gamma^4/3\rho^2 = 2e^2cE^4/3\rho^2(m_0c^2)^4,$$

where m is the mass of the electron. As shown in Fig. 8, the peak of the emitted energy spectrum increases with E. Note that power emitted is proportional to the inverse fourth power of the electron (or positron) mass, which is the reason that electrons (positrons) rather than heavier particles are used to produce synchrotron radiation.

Early synchrotrons were used primarily for particle physics, and synchrotron radiation was an undesired energy-loss mechanism. Any research done with the x rays was parasitic. These facilities have been called the first generation of synchrotrons. A second generation of synchrotrons was dedicated to the production of synchrotron radiation. In these facilities, electrons are held for many hours in a storage ring, providing a steady source of x rays for research. Figure 9a shows schematically some characteristics of the first- and second-generation synchrotron facilities.

A new, third generation of synchrotrons (see Fig. 9b) is presently under construction and will come on line in the United States, Europe, and Asia, starting in 1993. These facilities are characterized by small electron-beam size, low electron-beam emittance, and long straight sections in which are placed undulators and wigglers, so-called "insertion devices." The result will be x-ray beams of very high spectral brightness; several examples are shown in Fig. 10, along with a conventional x-ray tube. Brightness is defined as flux per unit area of the source, per unit solid angle of the radiation cone, and per unit bandwidth; thus, high brightness is

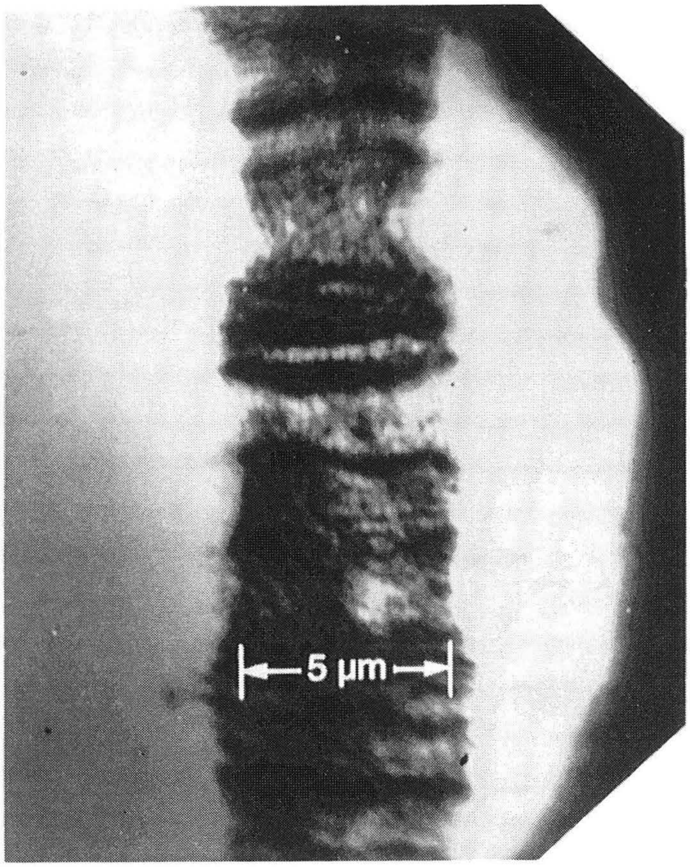

Figure 4. Image of a chromosome from a larva of the midge was obtained through x-ray microscopy. Although the banding structure can be seen through a visible-light microscope, an x-ray microscope was required to capture the filamentary structure between the bands. (Produced by G. Schmahl and M. Robert-Nicoud, University of Göttingen, at the BESSY synchrotron radiation facility, Berlin, Germany.)

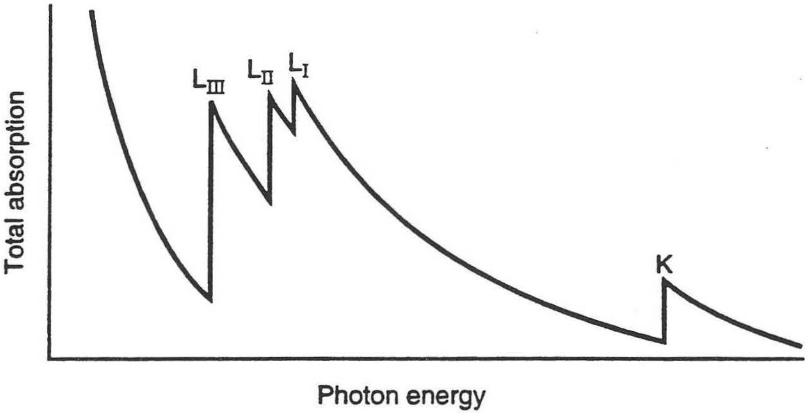

Figure 5. At absorption edges, the absorption of photons by an atom increases sharply because the photon energy is sufficient to remove an electron from a given shell of that atom. Thus photons can be used for element-specific detection and imaging.

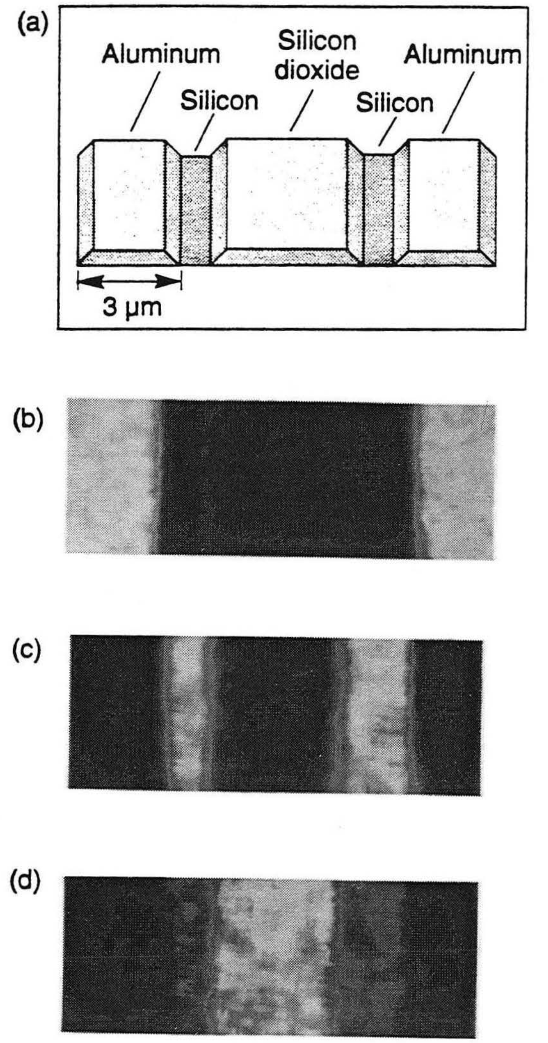

Figure 6. The chemical composition of a microfabricated sample (a) was determined through a technique called spectromicroscopy. After absorbing x rays, the sample emitted electrons with energies characteristic of its components. Analysis of these energies identified and mapped sections of aluminum (b) and pure silicon (c). Silicon atoms in silicon dioxide molecules (d) were mapped at a different location from pure silicon, indicating two distinct chemical states of silicon. (Based on work done by scientists from the State University at Stony Brook, IBM, and the Lawrence Berkeley Laboratory. Data were taken at the National Synchrotron Light Source, Upton, NY.)

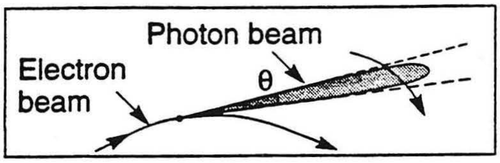

Figure 7. A beam of electrons travelling in a curved path at nearly the speed of light emits photon beams. The beams fan out at angle θ, the natural emission angle.

characterized by a high flux of radiation into a small spot and with a small spectral bandwidth. Undulators and wigglers both produce high flux (number of photons delivered per second). In the past, order-of-magnitude increases in brightness have led to qualitatively new developments in spectroscopic and structural studies of both gas-phase and condensed matter. No less is expected at these third-generation synchrotron facilities.

3. Third-Generation, Low-Energy, Synchrotron-Radiation Facilities

Several modern, low-energy, synchrotron-radiation facilities are presently planned or under construction around the world. Figure 11 shows their locations and domains of brightness compared with existing facilities. Table 1 lists important parameters for four low-energy facilities.

One example of a third-generation, low-energy synchrotron-radiation facility is the Advanced Light Source (ALS). At the ALS, an electron gun shoots electrons into a linear accelerator (or linac), which accelerates them to an energy of 50 MeV. The linac then injects the electrons into a booster synchrotron for further acceleration—to 1.5 GeV. At this energy, the electrons are moving at 99.999996% of the speed of light. From the booster, the electrons enter a storage ring with a circumference of 200 meters, where they circulate for hours at constant energy.

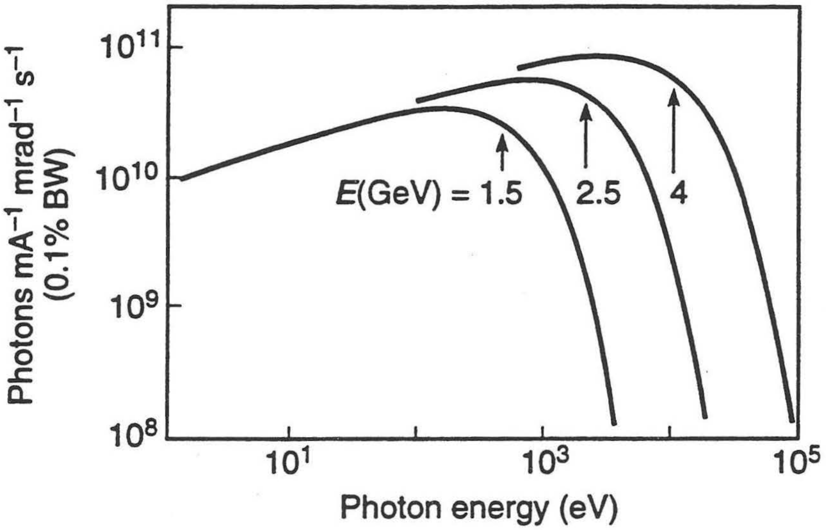

Figure 8. Photon emission as a function of photon energy for electrons (positrons) with an energy E of 1.5, 2.5, and 4 GeV. Maximum photon energy increases with increasing electron energy.

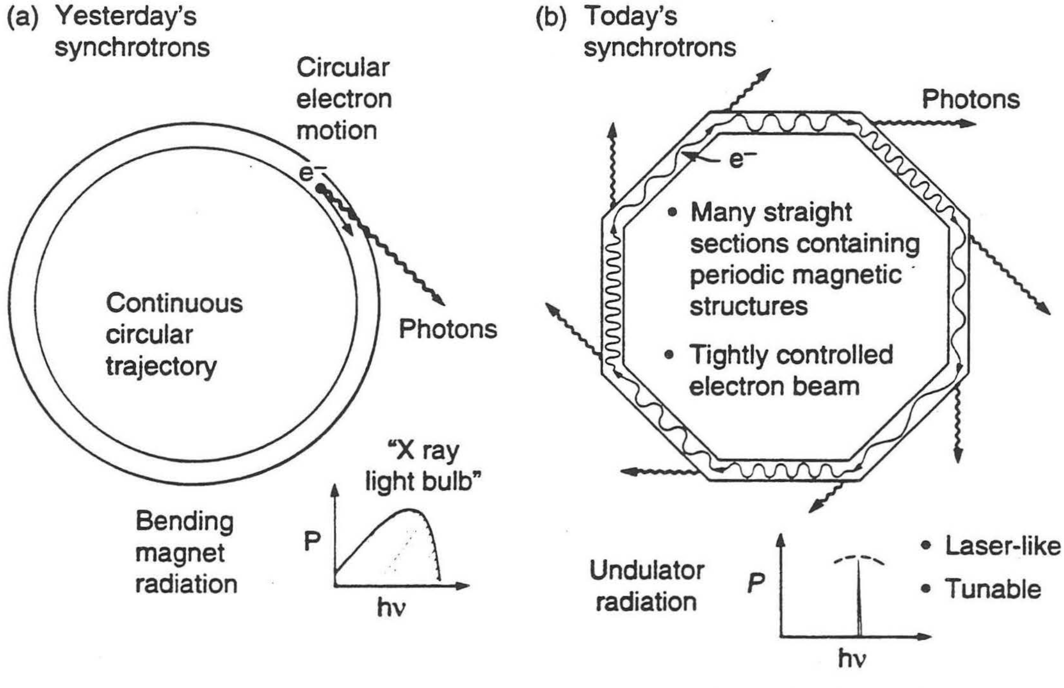

Figure 9. Evolution of synchrotron-radiation facilities: (a) characteristics of early synchrotrons versus (b) third-generation facilities.

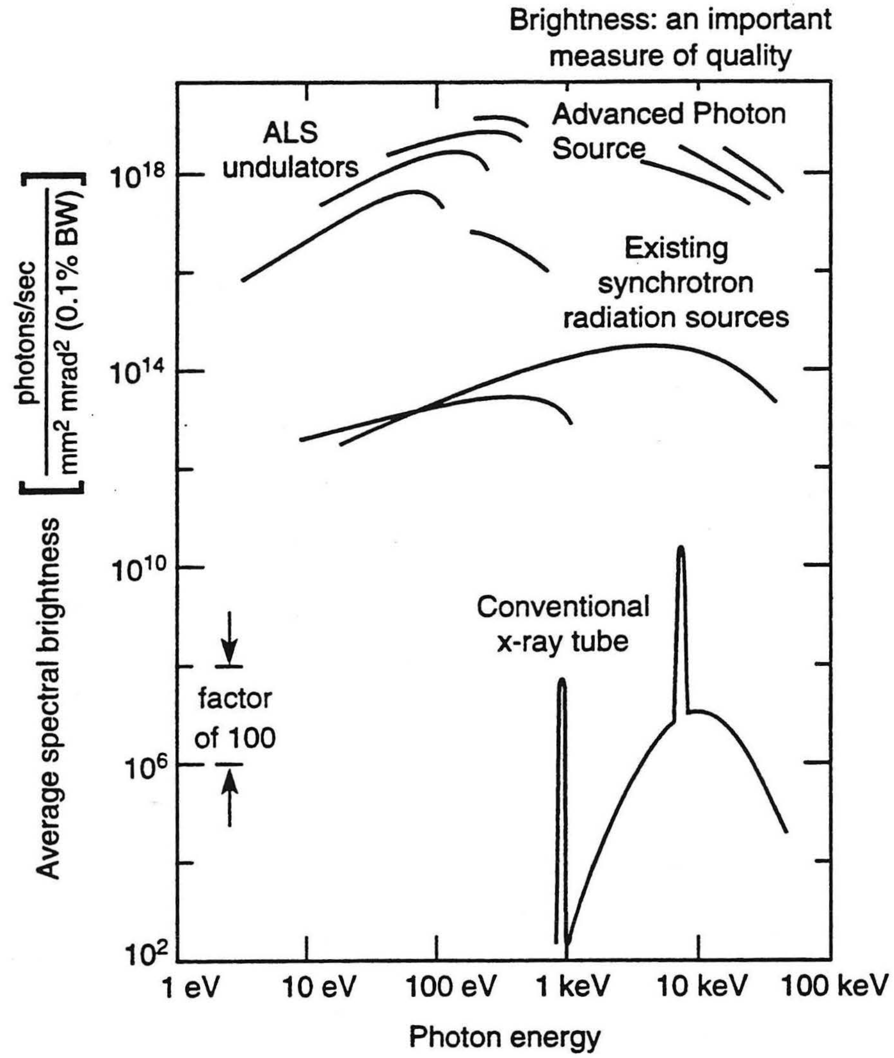

Figure 10. Spectral brightness as a function of photon energy for sample modern synchrotron-radiation sources (ALS and APS) and a conventional x-ray tube. Third-generation synchrotron-radiation sources are characterized by the high brightness of the light they deliver.

In the storage ring, the electron beam travels through a vacuum chamber in a sequence of 12 arc-shaped sections alternating with 12 straight sections. The arc sections are imbedded in a lattice of bending magnets and focusing magnets that force the beam into a curved trajectory and constrain it to a tight ellipse approximately 100 microns in vertical dimension in the straight sections. The three bending magnets in each arc have ports through which beams of synchrotron radiation pass as the electrons curve through the arc. Figure 12 shows the arc sections and magnet lattice.

The straight sections, which have no focusing or bending magnets, are used for other purposes. One is the site of electron injection from the booster. Another is surrounded by radio-frequency (rf) cavities in which electromagnetic fields oscillate at a frequency of 500 MHz. These fields

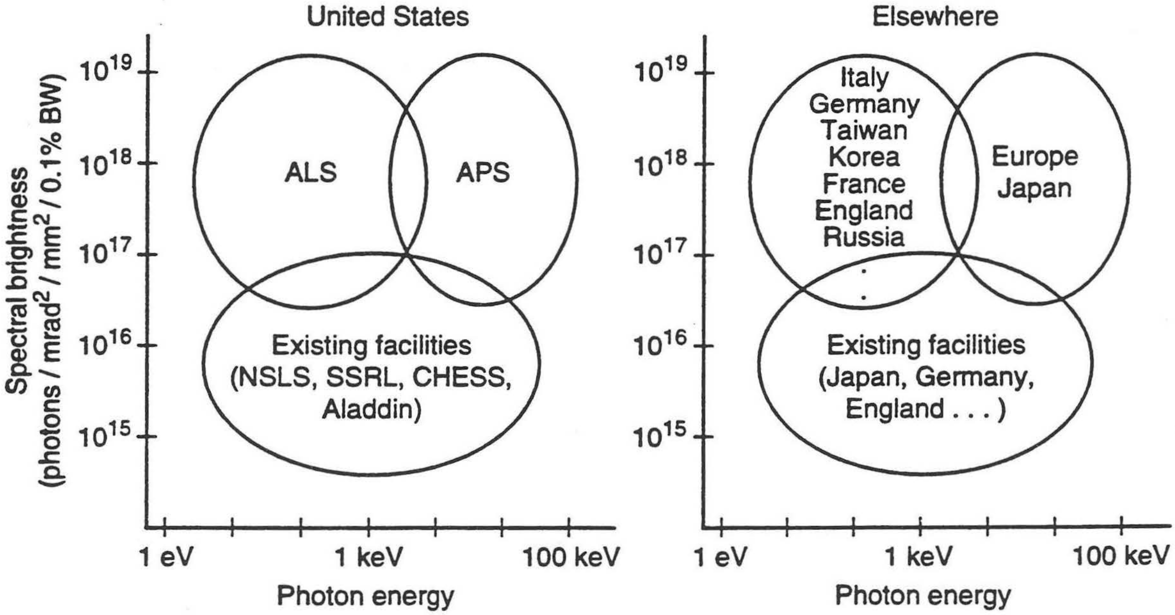

Figure 11. Many low- and high-energy synchrotron-radiation sources have been built or are under construction around the world. The light delivered by third-generation, low-energy, synchrotron-radiation sources will be up to several order of magnitude higher than that from existing facilities.

Table 1. Salient parameters for four third-generation, low-energy, synchrotron-radiation facilities.

	Super ACO	ALS	ELETTRA	SOLEIL
Energy	0.8 GeV	1.5 GeV	1.5–2 GeV	2.15 GeV
Circumference	72 m	197 m	259 m	200 m
Emittance	35 nm rad	< 10 nm rad	4–7 nm rad	17–36 nm rad
Critical energy	0.66 keV	1.56 keV	1.36 keV	5 keV
Critical wavelength	18.6 Å	7.9 Å	9.1 Å	2.5 Å
Particle	positron	electron	electron	positron
Injector	linac	synchrotron	linac	synchrotron
Straight sections	6	10	11	12
Undulator length	3.2 m	4.5 m	6 m	4-5 m
Bunch length	100 ps	35–50 ps	12–20 ps	70–80 ps
Bunch number	24 max	250 max	432 max	240 max
Beam lifetime	6 hours	4–6 hours	4–10 hours	14–24 hours
Begin operation	1988	1993	1995	2000

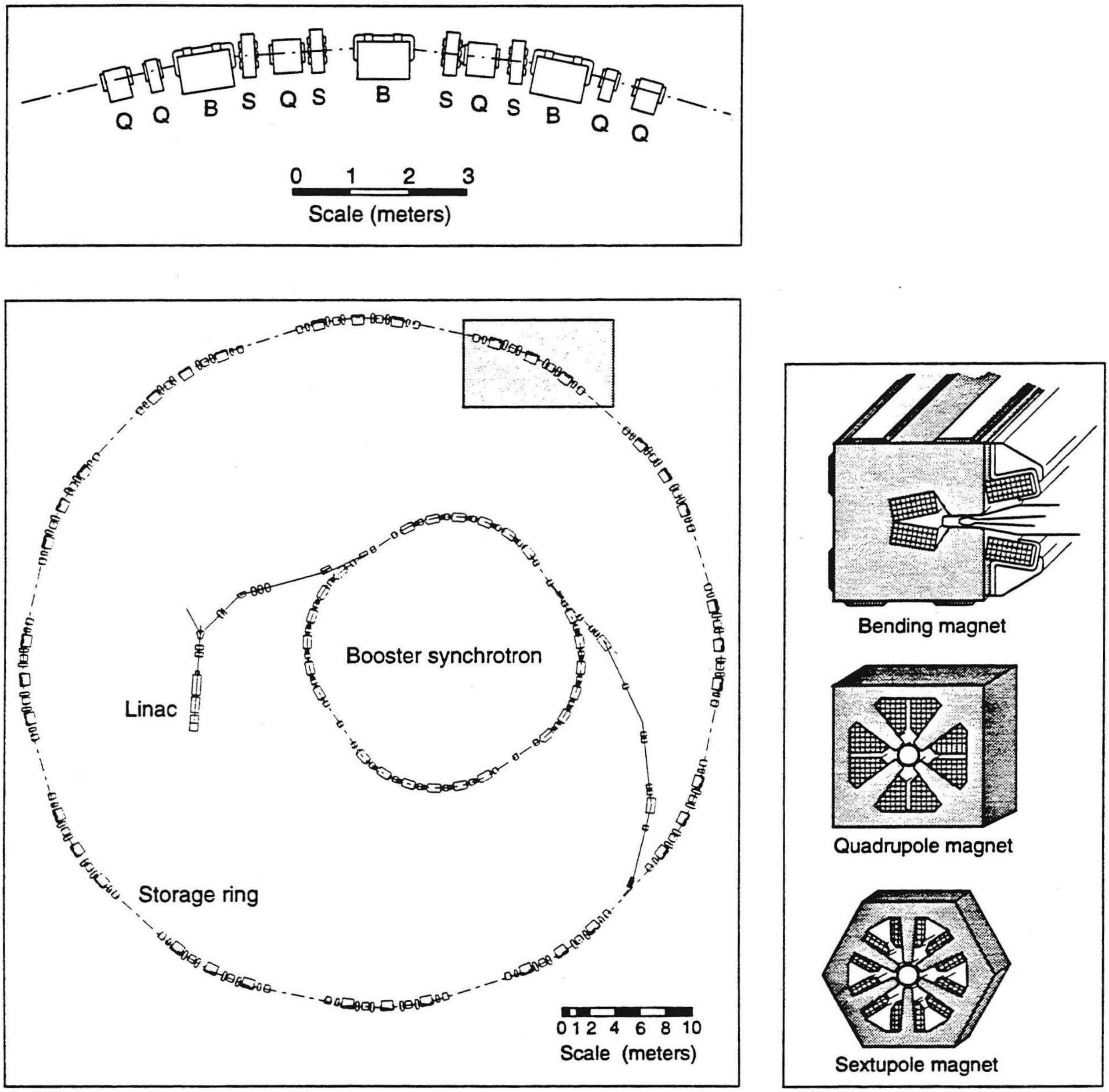

Figure 12. The ALS storage ring has 12 arc-shaped and 12 straight sections. The arc sections are imbedded in a magnetic lattice, which consists of 12 magnet sequences, one for each arc. Each sequence contains three bending magnets (B), six quadrupole magnets (Q), and four sextupole magnets (S). Relativistic electrons, accelerated by the linac and booster synchrotron, travel through the storage ring generating synchrotron radiation.

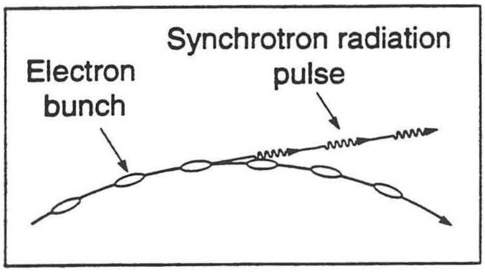

Figure 13. Schematic illustration of the bunched structure of an electron beam circling in a storage ring and the corresponding pulsed nature of the synchrotron radiation. At the ALS, for example, 250 electron bunches circle the ring. Each has a duration of about 35 picoseconds. The spacing between bunches, dictated by the rf frequency, is 2 nanoseconds.

replenish the electron-beam energy lost to synchrotron radiation. Synchrotron radiation emitted by the bunched electron beam is not emitted continuously but in a pulsed fashion, as shown in Fig. 13.

The 10 remaining straight sections at the ALS are designed to accommodate devices called undulators and wigglers, which generate synchrotron radiation with enhanced characteristics. Collectively termed "insertion devices," undulators and wigglers consist of a linear array of north-south magnetic dipoles of alternating polarity (see Fig. 14). The normal vertical orientation of the dipoles causes relativistic electrons of energy E to undergo a nearly sinusoidal electron trajectory of period l_u in the horizontal plane, causing the emission of synchrotron radiation. The peak magnetic field B_0 on the undulator axis depends exponentially on the ratio R of the gap between the dipole north and south pole faces g to the period of the undulator l_u. For hybrid devices made with the permanent-magnet material neodymium-iron-boron, B_0 is approximately

$$B_0[\text{Tesla}] = 3.44\, e^{-R(5.47-1.8R)}$$

for $0.07 < R < 0.7$.

The deflection parameter K is the ratio of the maximum angular deviation of the electron trajectory from the insertion-device axis to the natural opening angle of the synchrotron-radiation cone. The cone has a natural opening angle that is inversely proportional to the electron-beam energy. Expressed in terms of undulator parameters, K is approximately

$$K = 0.934\, B_0[\text{Tesla}]\lambda_u[\text{cm}]\,.$$

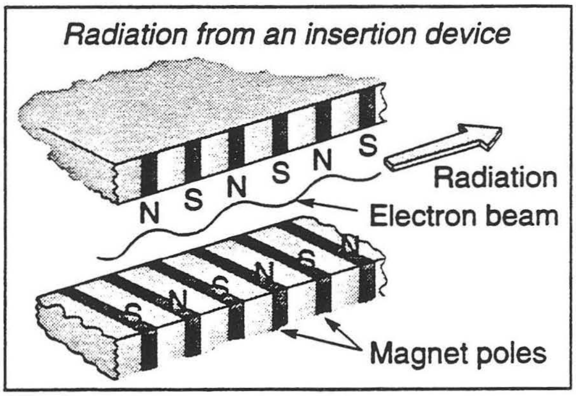

Figure 14. An insertion device has permanent magnets of alternating polarity that cause electrons moving at nearly the speed of light to follow a sinusoidal path perpendicular to the magnetic field.

A K value around 1 defines the breakpoint between an undulator and a wiggler. However, an insertion device retains significant undulator properties at higher K values, and most of the undulators planned for the new synchrotron sources operate in this intermediate range with $K > 1$. When $K >> 1$, the structure is called a wiggler.

In the undulator regime, an important effect comes into play that gives insertion devices special properties. Because of the rather gentle perturbation of the electron trajectory in an undulator (several micrometers amplitude), the electron trajectory during a pass through the device lies within one radiation-cone opening angle. This condition means that the radiation emitted from successive undulator periods adds coherently. The interference behavior due to the coherence gives rise to a sharply peaked radiation spectrum consisting of a fundamental and several harmonics. The photon energy ε_n of the nth harmonic is

$$\varepsilon_n[\mathrm{keV}] = \frac{0.949 n E^2[\mathrm{GeV}]}{\lambda_u[\mathrm{cm}]}\left(\frac{1}{1+K^2/2+\gamma^2\theta^2}\right),$$

where γ is the ratio of the electron relativistic and rest masses and θ is the angle of emission relative to the undulator axis. By contrast, the lack of interference in a wiggler means that its synchrotron-radiation spectrum is like the broad, continuous spectrum from the dipole or bending magnets in the curved sections of the storage ring.

It is important to the experimenter to be able to select the photon energy of the undulator light—that is, the light should be tunable. In principle, the photon energy is tuned from high to low values primarily by decreasing the undulator gap g from a maximum to a minimum distance, thereby increasing the field B_0 and the value of K. Both the minimum and the maximum energies are arbitrarily set by the drop-off of the photon flux at low and high gap values, but are also subject to constraints such as the vertical diameter of the storage ring vacuum chamber. At the ALS, use of the third and fifth harmonics of the undulators is planned to extend their spectral range to higher photon energies than can be reached with the fundamental alone.

While tunable, undulators retain their most desirable properties in a comparatively small photon-energy range. For $K << 1$, the only significant photon flux is in the fundamental. As K is increased, the number of harmonics with measurable photon flux grows rapidly. It becomes useful to define a critical harmonic n_c above which half the total radiated power occurs. The critical harmonic is given by

$$n_c = 0.75K\left(1+\frac{K^2}{2}\right) .$$

The cubic dependence of n_c on K means that most of the undulator radiation is in the harmonics when tuning the undulator to lower photon energies. Essentially, increasing K too far turns the undulator into a wiggler, as the higher harmonics blend together into a broad spectrum.

A summary of the properties of undulator and bending-magnet radiation is shown in Figs. 15 and 16, in which the data apply to the ALS. The undulator radiation is seen to have both spatial and spectral properties, which enhance its usefulness for research.

Low-emittance storage rings and insertion devices have created new challenges for designers of XUV optics. First, the source size and divergence have become smaller. For ALS undulators at the high-photon-energy end of the spectral range, the rms size is typically 330 μm horizontal by 65 μm vertical and the rms divergence is typically 40 μrad horizontal by 30 μrad vertical. The smaller source size requires tighter tolerances for relay optics and monochromator components in both optical figure and finish to avoid loss of light (e.g., rms surface roughness ≈ 0.5 nm and tangential slope error <1 μrad for a condensing mirror). The attainment of higher resolution by the use of smaller slits also becomes practical (the spectral-resolution goal of monochromators in undulator beamlines is $\Delta E/E \approx 10^{-4}$). Monochromator components, therefore, need tighter tolerances to avoid loss of resolution. Finally, the photon-beam power is several kW/cm^2. The

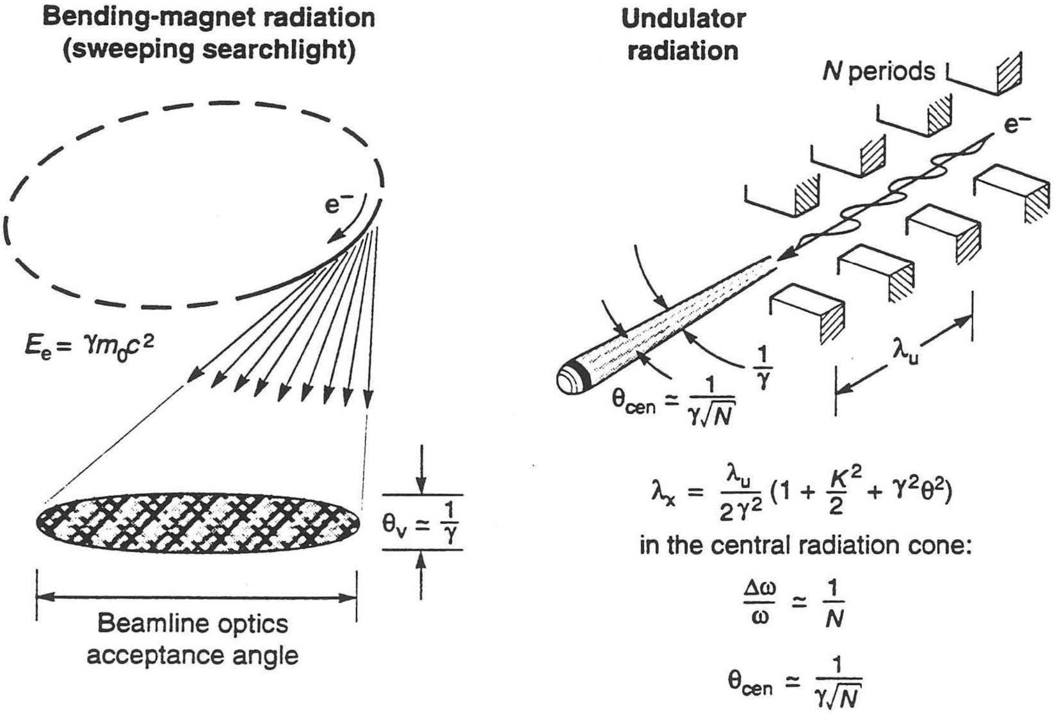

Figure 15. Characteristics of the synchrotron radiation produced by bending magnets and undulators.

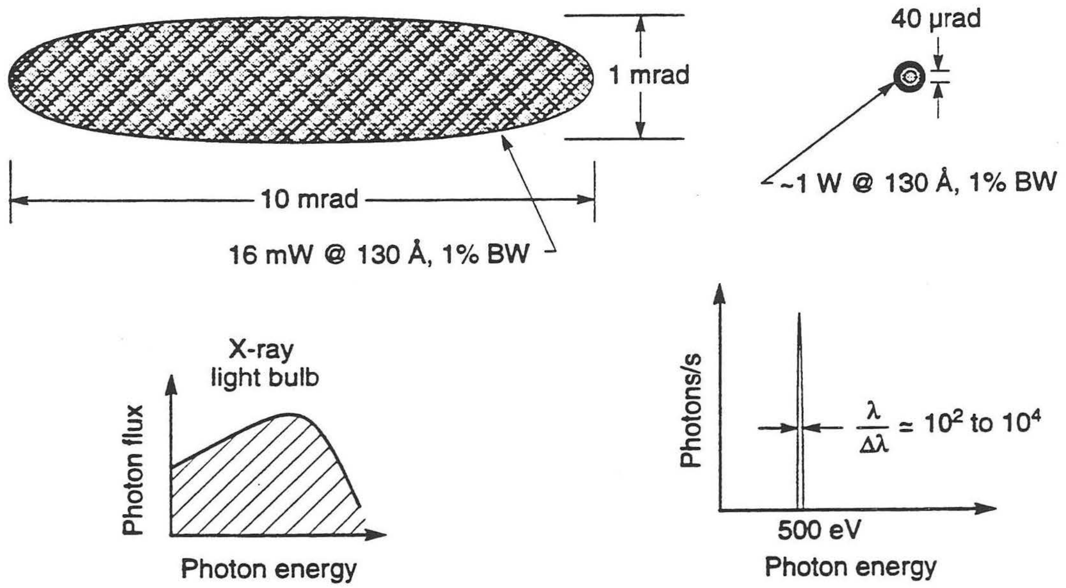

Figure 16. Angular divergence and spectral distribution of bending magnet and undulator radiation. The data apply to the ALS.

requirement that thermal distortions and stress be controlled complicates the design [for example, water cooling in a UHV (≈ 1 ntorr) environment is required] and limits the choice of materials.

The most serious limitation is that of optical fabrication tolerances. It is difficult to fabricate aspheric optical surfaces (such as paraboloids, ellipsoids, and toroids) sufficiently accurately in mirrors, monochromators, and other optical elements to take full advantage of the undulator source. One way to address this problem is to avoid the use of aspheric surfaces and to build beamlines entirely with plane and spherical surfaces.

4. Special Characteristics of Synchrotron Radiation

Synchrotron radiation has certain characteristics that, individually or combined, allow researchers to perform experiments not otherwise possible:

- Very high brightness
  - high spatial resolution
  - high spectral resolution
- Tunability
- High degree of coherence
- A pulsed nature
- Linear or circular polarization
- High flux.

Of these, the most prized characteristic is *high brightness*: the light has a high photon flux per unit source area and per unit solid angle into which the source radiates.

A major benefit of brightness is *high spatial resolution* (or focusability). High spatial resolution is achieved because many photons can be focused on an extremely small spot, in which they can generate characteristic absorption, photoelectron, or other types of spectra. In many cases, the smaller the focal spot, the smaller the object that can be distinguished from its surroundings. With help from special optical devices, a third-generation light source like the ALS is expected to achieve spot sizes as low as 200 Å in diameter (see Figs. 17 and 18).

High spectral resolution is a second major benefit of high brightness. High brightness allows a major portion of the photon beam to be focused through the monochromator slits, thereby increasing the resolution at fixed measurement time or decreasing the measurement time at fixed resolution. High spectral resolution is useful for separating chemical shifts and for resolving narrow spectral features.

Chemical shifts can be used to determine the chemical state of atoms in solids. For example, measurement of the electron-energy spectrum emitted by photons hitting Si(100) with a 5-Å surface of SiO_2 allows the oxidation state of Si in the interface region to be determined (see Fig. 19). An example of imaging with chemical-state selectivity has been shown in Fig. 6.

Another example of the use of high spectral resolution is in measuring narrow spectral features. For example, resonant states of the He atom were first measured in 1963 by Madden and Codling, as shown in Fig. 20. These resonant states exhibit the characteristic Fano profile arising from interference between two paths to reaching the same final state. With improved resolution and much higher photon fluxes, many additional states can be seen in the ionization spectrum of He (1992 measurement also shown in Fig. 20).

Higher resolution can yield even more information, as shown in the more detailed spectrum in Fig. 21. The spectral region between two peaks (3+ and 4+) is seen to contain an additional small

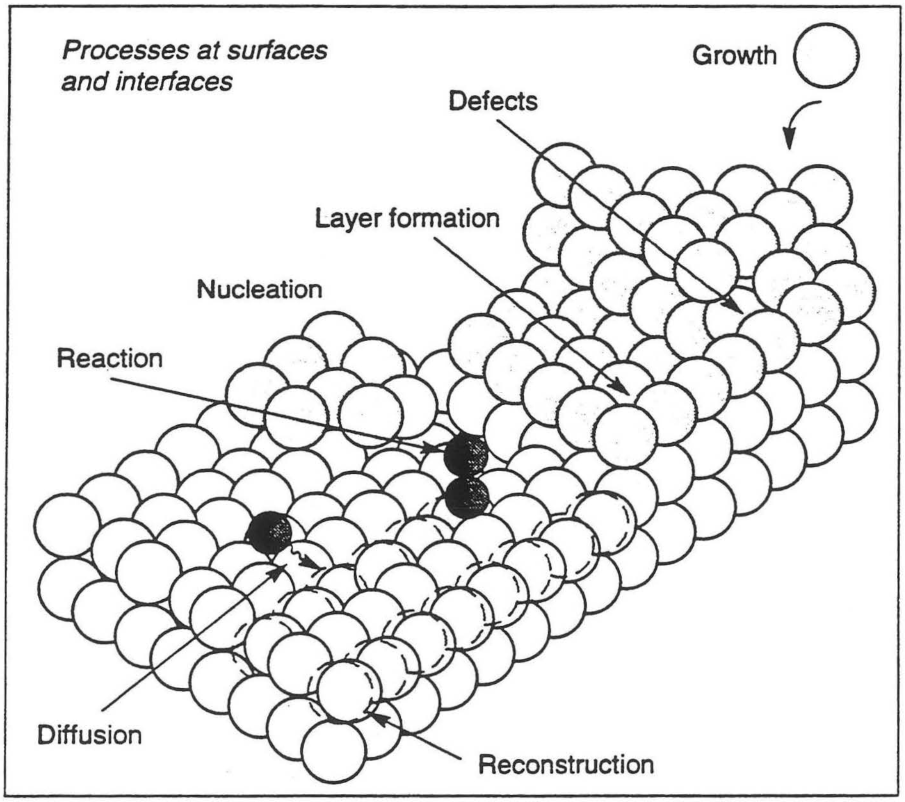

Figure 17. Many physical, chemical, and biological processes occur at solid surfaces and interfaces between materials. With light from third-generation synchrotron sources, scientists can study surface areas only 200 Å in diameter. By using techniques such as microprobe analysis or x-ray microscopy, they can obtain information about the growth of layers on the surface, reactions, diffusion, nucleation, and defects (missing or misplaced atoms) in such small areas.

peak (4–) and an even smaller peak (2p3d) next to it. These peaks and the physics underlying them could not be accessed without very high spectral resolution.

Apart from the issue of spectral resolution, the *tunability* of synchrotron radiation is important in itself. From the range of available wavelengths in a beam, one can select a specific wavelength (or photon energy). A wavelength would be selected, for example, because an atom in a sample exhibits a sharp increase in the absorption of light at this wavelength. X-ray absorption spectroscopy, a family of analytical techniques based on the absorption of light by atomic species, can reveal the identity, electronic structure, and chemical bonding state of the absorbing atom and provide information about the identity, number, and arrangement of the atoms around it.

A significant fraction of the long-wavelength radiation from undulators in a third-generation synchrotron is *spatially coherent*. The criterion for spatial coherence is that the product of the area of the light source and the solid angle into which it emits must be no larger than the square of the wavelength of the light. Since this is the diffraction condition, spatially coherent light is also said to be diffraction-limited. In accordance with the diffraction condition, the electron-beam emittance e sets the minimum wavelength at which all the radiation can be diffraction-limited, according to the relation

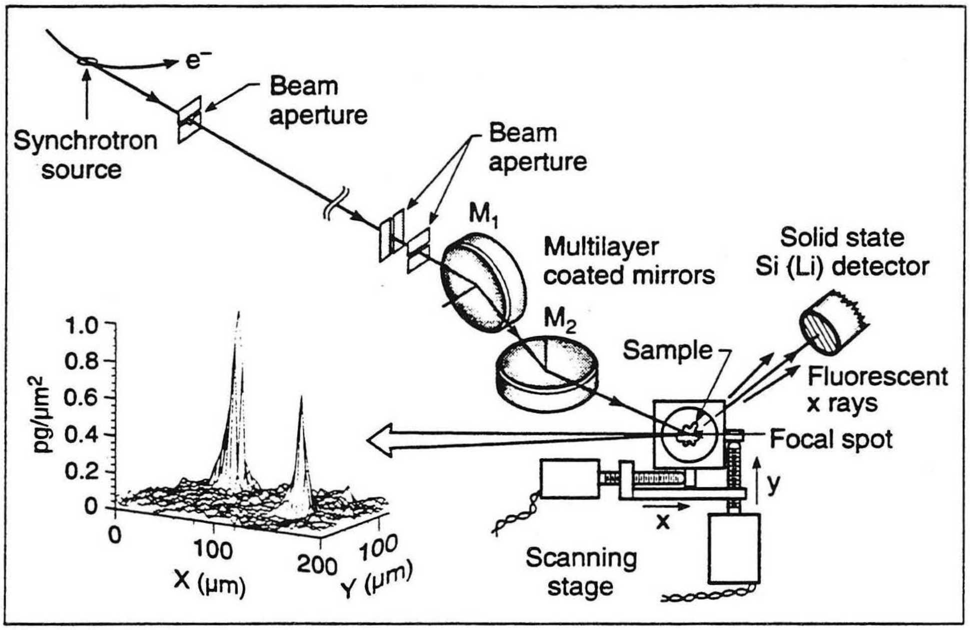

Figure 18. Diagram of an x-ray microprobe built at Lawrence Berkeley Laboratory shows how a pair of grazing-incidence mirrors coated with multilayers can be used to focus a beam of x rays to a spot several microns in diameter. The beam apertures further reduce the spot size to about 2 µm. The three-dimensional graph illustrates the capability of the microprobe to detect trace amounts of impurities. In this example, the tall peaks represent iron impurities detected in a silicon carbide ceramic substrate. They came from stainless steel tweezers used to handle the ceramic. (The data were taken at the National Synchrotron Light Source by A. Thompson and K. Chapman of Lawrence Berkeley Laboratory.)

$$e = l_{\mathrm{min}}/4p \ .$$

Even at wavelengths below the minimum, part of the radiation remains diffraction-limited, the fraction decreasing as the square of the wavelength.

Although not as coherent as the visible light from most lasers, undulator radiation has much more coherence than ever before available in the vacuum ultraviolet and soft x-ray regions of the spectrum. One of the most exciting uses for coherent synchrotron radiation is holography (see Fig. 22). While laser light can be used to make holograms of objects that we can see, coherent x rays can image objects that are far smaller.

A more general virtue of coherent radiation is the ability to focus. For example, a Fresnel zone plate can focus a coherent beam of soft x rays to a spot with a radius approximately 1.2 times the width of the outermost zone. With state-of-the-art microfabrication techniques, such as electron-beam holography, it is possible to make zone plates with outer zone widths of about 300 Å. This capability can be exploited in scanning or imaging systems to generate spatially resolved information with a comparable resolution.

Coherent synchrotron radiation can also be used to test the quality of optical lenses and mirrors used in x-ray applications—for example, x-ray astronomy, x-ray lithography for manufacturing microchips, and x-ray imaging of microstructures in biology and materials science. The smaller

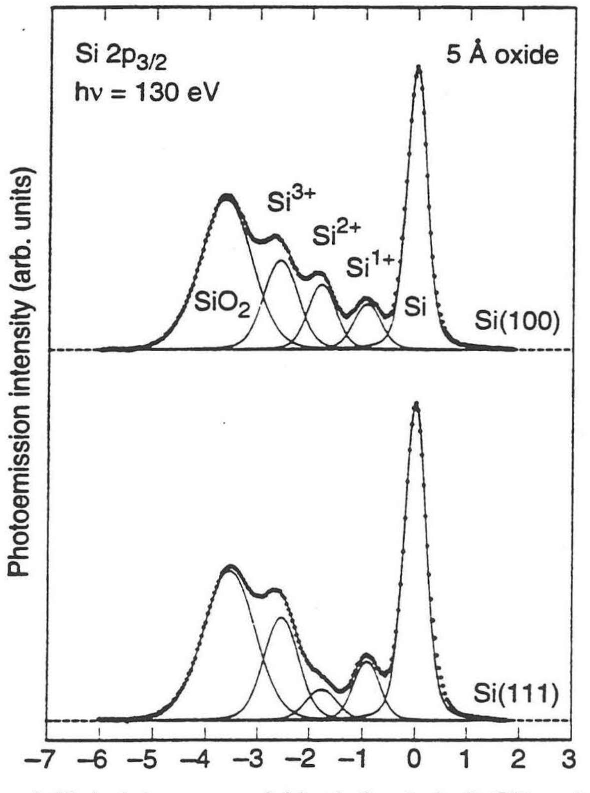

Figure 19. Photoemission from Si(100) with a 5-Å oxide surface, shown as a function of initial-state energy. The oxidation states of Si are shown to be resolved. From Himpsel, McFeely, Taleb-Ibrahimi, Yarmoff, and Hollinger, Physical Review B **38**, 6084 (1988). (Measurements made at the National Synchrotron Light Source.)

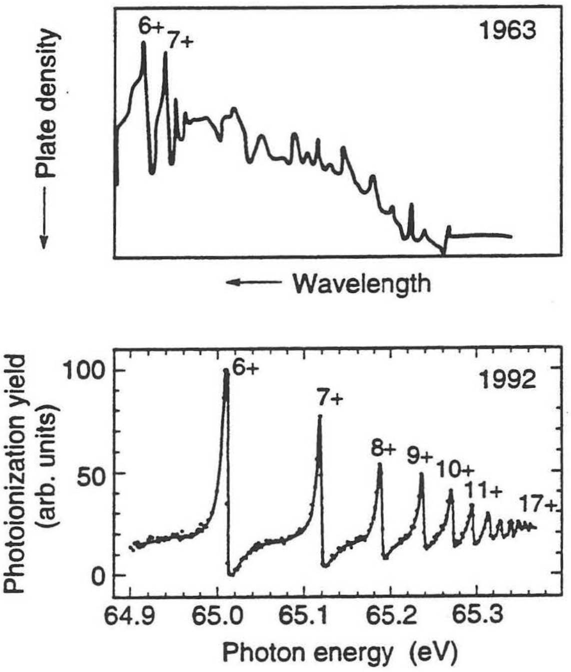

Figure 20. Synchrotron radiation absorbed at certain photon energies ionizes helium gas atoms and excites the helium ions to a series of distinct quantum states (as revealed by the peaks). The high resolution and capability to tune the radiation to the discrete photon energies required for excitation allowed the quantum states to be seen. This figure demonstrates the improvement in resolution since the pioneering work of Madden and Codling in 1963, in which the series of peaks was first observed. (Measurements in 1992 made by Z. Hussein, T. Reich, D. Shirley, et al., at Stanford Synchrotron Radiation Laboratory.)

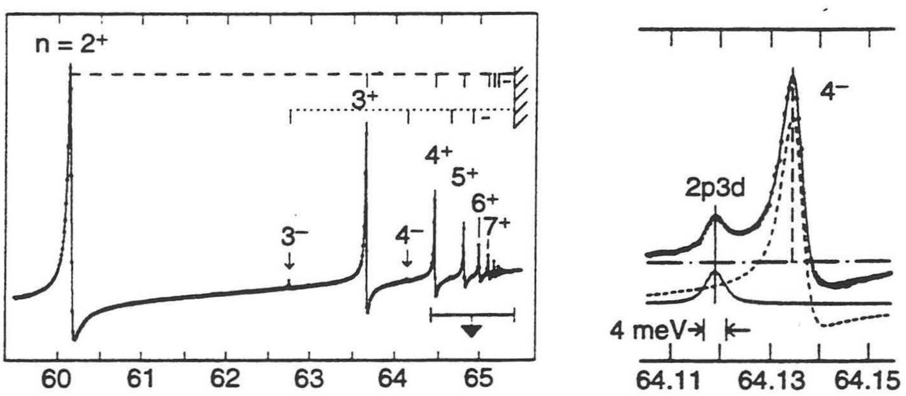

Figure 21. Doubly excited states of He^+ lying below the $n = 2$ threshold, including three Rydberg series, have been observed. The 2p3d peak is 4 meV wide, demonstrating the excellent spectral resolution. From Domke *et al.*, Physical Review Letters **69**, 1171 (1992). (Measurements made at BESSY.)

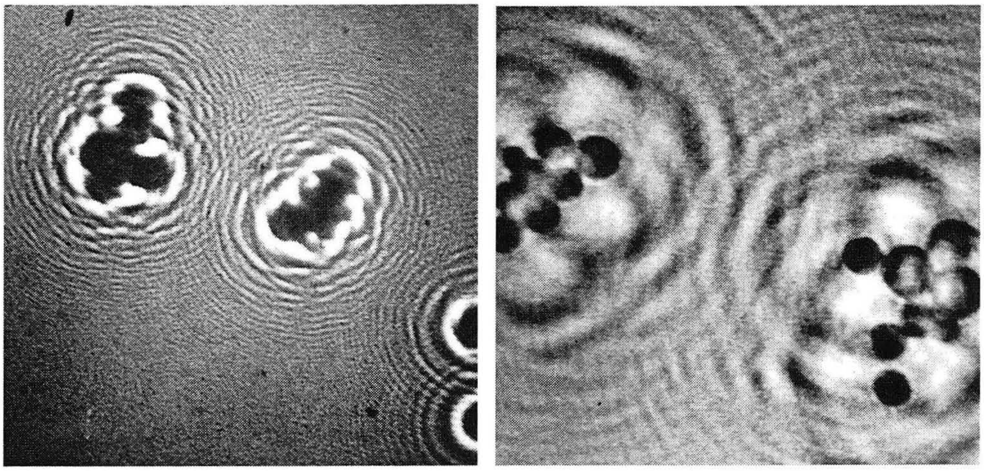

Figure 22. The ripple-like pattern in the x-ray hologram (left) contains the information needed to create the reconstructed image (right) of zymogen granules, which appear as dark spherical objects. These are storage vesicles for digestive enzymes found in a pancreatic cell. Such images can reveal information about digestion mechanisms. The shading of the zymogen granules indicates their density. The darker a granule, the more dense it is, indicating a larger enzyme content. (Produced by Stephen S. Rothman, Malcolm Howells, Chris Jacobsen, and Janos Kirz at the National Synchrotron Light Source, Brookhaven National Laboratory.)

the object imaged, the greater the demand for high-quality optics polished to eliminate virtually all defects. Figure 23 shows the principal tool to be used at the ALS for testing x-ray optics for lithography.

Time resolution, a feature of all synchrotron sources, follows from the bunched character of the electron beam in the storage ring. Standard pulses delivered by the ALS are 35 ps wide at half maximum and occur at intervals of 2 ns. This time structure can be varied by injecting only one or a few electron bunches into the storage ring. In this few-bunch mode, the ALS delivers pulses at longer intervals.

The time structure of synchrotron radiation can be used for a variety of timing experiments. The structure is different from that of a laser in that the synchrotron radiation has a low energy per pulse but a very high repetition rate (500 MHz for the ALS); therefore, the time-averaged power is high. Because the per-pulse power is low, harmonics cannot be generated with the UV photons produced by a storage ring; however, an undulator can directly produce harmonics.

The pulsed nature of synchrotron radiation can be used to observe short-lived or transient systems by means of time-resolved spectroscopic, scattering, and imaging experiments. For example, if radiation damage due to x-ray exposure can be avoided or minimized, it might be possible to image changes in functioning biological cells and cellular structures in near-natural environments. Also, one might study the kinetics of a chemical reaction or the lifetime of excited states of atoms or molecules (see Fig. 24). The ultimate time resolution, possible only if there are enough photons in a single pulse of bright synchrotron light to generate a useful signal, would be to follow events in real time on the sub-nanosecond time scale.

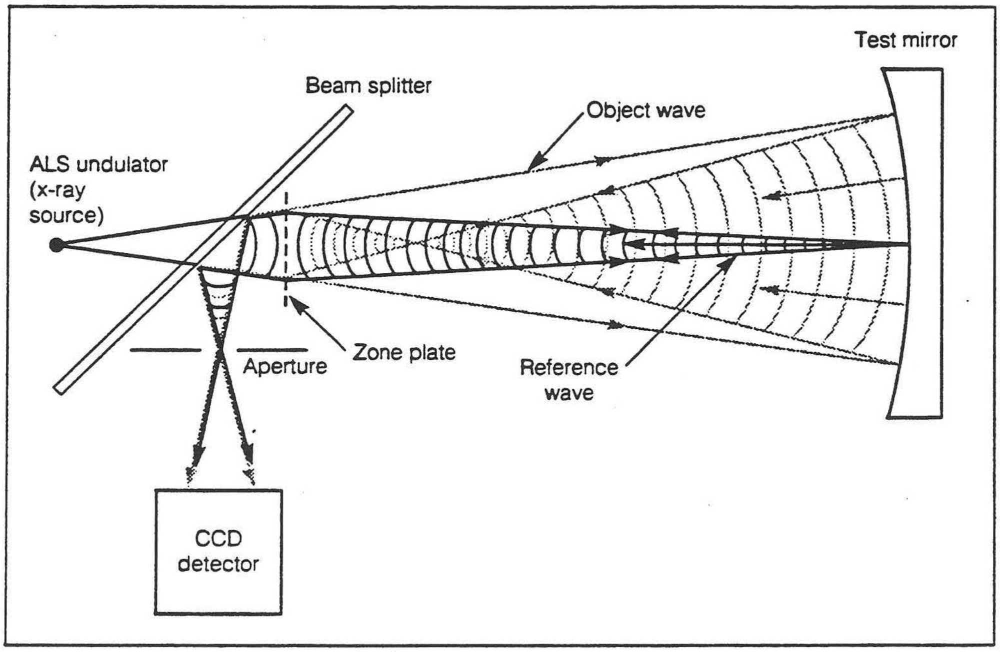

Figure 23. The main tool for determining the quality of optics is an interferometer. Coherent x rays are directed through this device onto the object being tested. Inconsistencies in the curvature or smoothness of its optical surface cause the reflected x rays to change phase with respect to reference x rays from the same source, which do not change phase. The phase difference between the object and reference waves provides a measure of the quality of the optic.

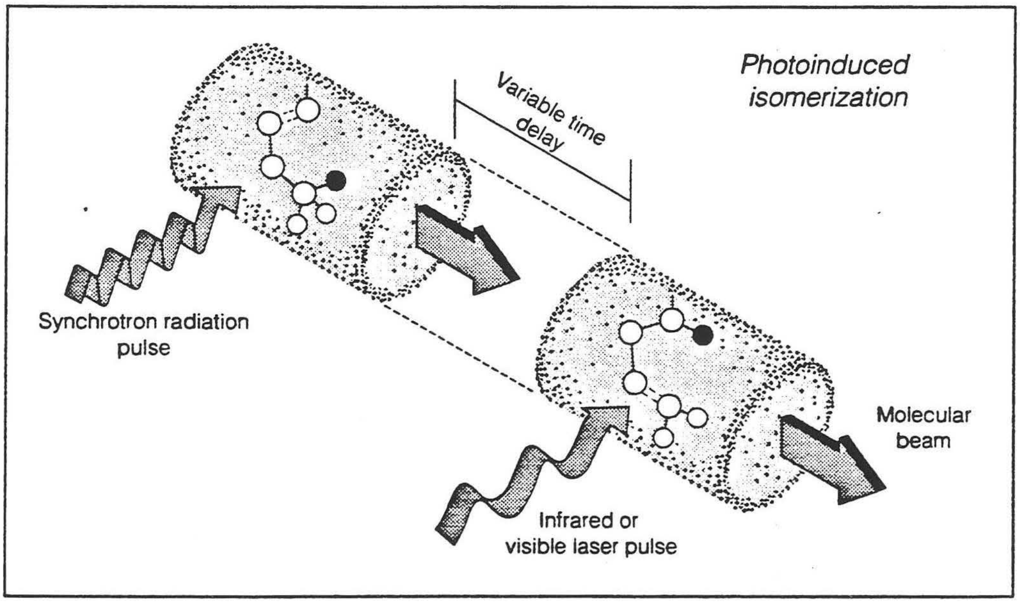

Figure 24. The kinetics of chemical reactions can be investigated with pulsed light from two sources in "pump-probe" experiments. A pump pulse of synchrotron radiation initiates a chemical reaction that is interrogated by a probe pulse from a laser.

Time resolution can also be achieved by operating in synchrony with other light sources, such as a high-speed laser in a pump-probe mode. The extremely narrow width and rapid frequency of the standard pulses make it possible to investigate ultrafast processes, whereas the ability to lengthen the interval between pulses would allow the study of processes with relatively long lifetimes.

Polarization control is another feature that is associated with synchrotron sources. Undulator radiation is completely linearly polarized. Radiation from bending magnets is largely linearly polarized when viewed in the plane of the electron orbit, but it is elliptically polarized when viewed at angles above or below the plane. With special insertion devices, e.g., crossed-field undulators and elliptical wigglers, it is also possible to generate elliptically polarized beams, in particular, circularly polarized beams (see Fig. 25), which can be used to investigate structures with a handedness (chiral structures) and magnetic materials.

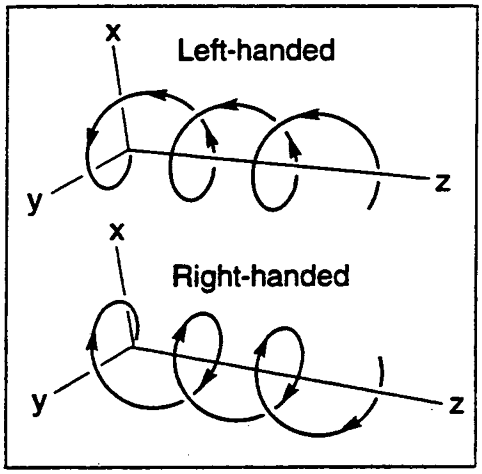

Figure 25. The unique property of circularly polarized light is the spiral path of its electric-field component. This component maps out a clockwise or counterclockwise circular path to form a right-handed or left-handed spiral.

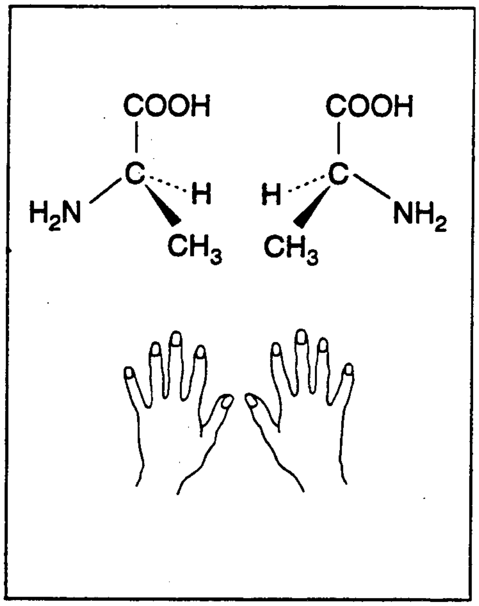

Figure 26. Like left and right hands, chiral molecules are mirror images that cannot be superimposed. The pair of chiral molecules shown here are examples of amino acids, the building blocks of proteins.

Polarized synchrotron radiation can be used to investigate anisotropic molecules—those that exhibit different responses to the light, depending on the direction of the *E*-vector. For example, one molecule of a chiral pair (see Fig. 26) might absorb more right than left circularly polarized light than its counterpart. An experiment based on this phenomenon could elucidate the molecular structures. Many biological molecules such as DNA or amino acids (the building blocks of proteins) lend themselves to experiments with polarized synchrotron radiation.

Because of their inherent directional spin, magnetic materials can also exhibit dichroism. Scientists have exploited this phenomenon by using circularly polarized synchrotron radiation in conjunction with an imaging microscope to obtain pictures of bits, as small as 10 μm × 1 μm, on a computer's magnetic storage disk (Fig. 27). It was possible to obtain these images because each bit corresponds to a magnetic region with its own direction of magnetization. This type of research can lead to a greater understanding of the magnetic characteristics of materials and possibly to the development of new materials with greatly increased magnetic storage capacity.

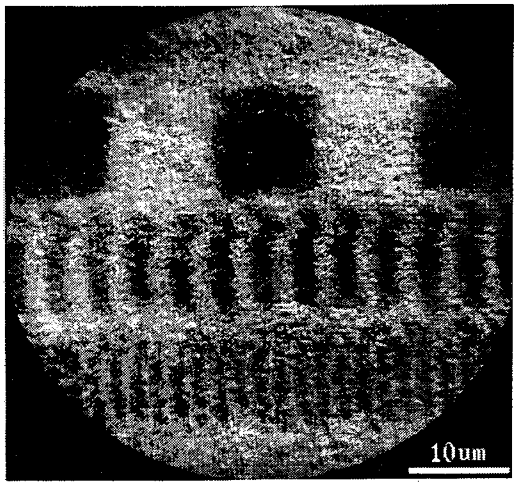

Figure 27. Image of magnetic bits on a storage disk was obtained by subtracting two images recorded with right circularly polarized synchrotron radiation tuned to the cobalt L_3 and L_2 x-ray absorption edges. The magnetization direction of the bits lies along the rows but points alternately to the right and to the left in the picture. The dimensions of the bits in the three rows are (from the top row, in microns) 10 × 10, 10 × 2, and 10 × 1. (Produced by scientists from the IBM Almaden Research Center and the University of Wisconsin, Milwaukee, at Stanford Synchrotron Radiation Laboratory, Stanford, CA.)

High flux is necessary for many experiments. For example, the number of atoms or molecules, such as impurities in a semiconductor or ionized atoms in a vapor, may be too small to generate a measurable signal in a practical time without sufficient photon flux. A high photon flux effectively compensates for the small number of signal generators by exciting them more often, thereby making impractical experiments feasible. An example of an experiment requiring high flux, but not particularly high brightness, is the photoionization of ions without narrow spectral features, as demonstrated by electron-spectroscopic measurements of Ca^+ ions (Fig. 28). The ion beam is large, and the width of the spectral feature observed is not narrow; hence, high brightness would not be important in this experiment. High flux, however, is essential because of the low density of the ions in the beam, resulting in a low signal rate.

Many additional types of experiments will utilize the properties of modern third-generation synchrotron light sources. An example is photoelectron holography (see Fig. 29). This figure shows a reconstruction of a copper lattice based on emitted photoelectrons, demonstrating spatial resolution on an atomic level.

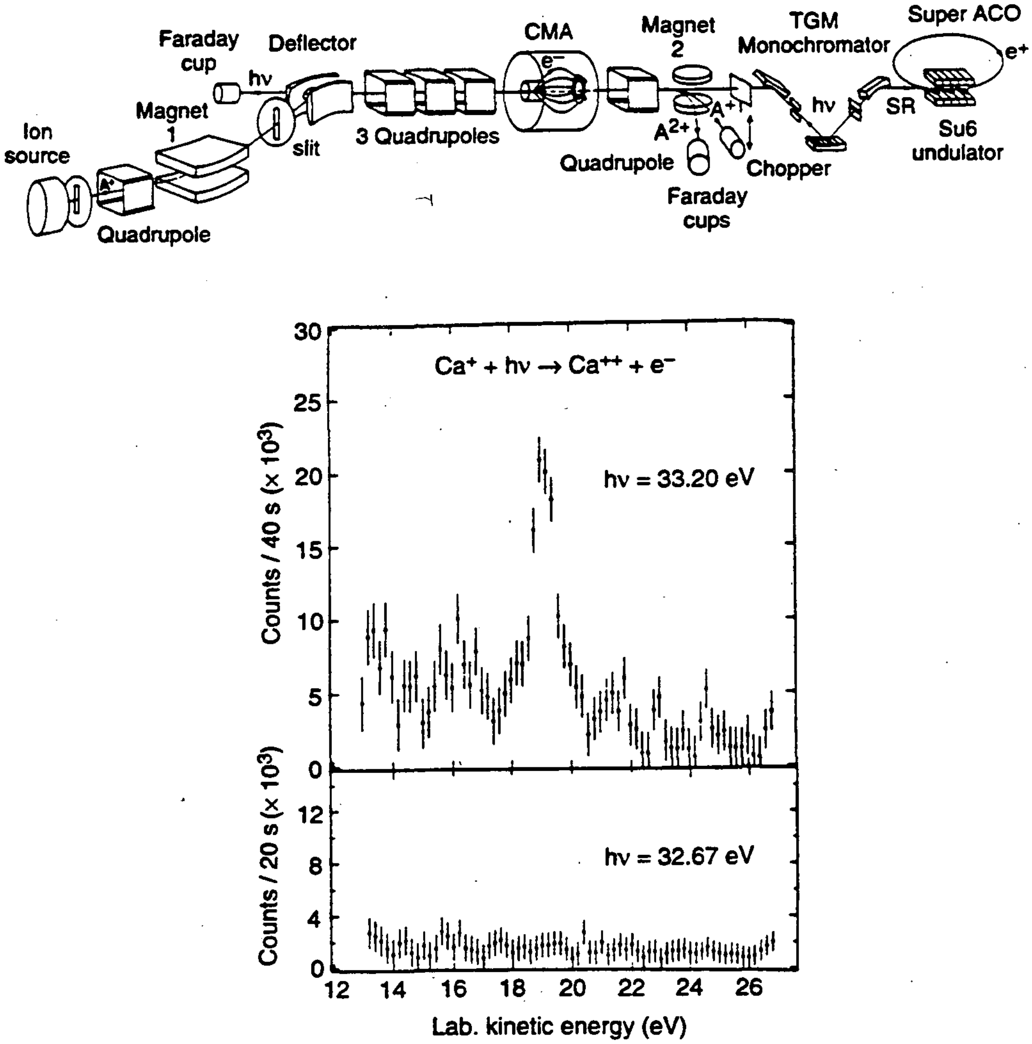

Figure 28. Apparatus used by Bizau *et al.* to measure the electron spectrum of photoexcited Ca^+ ions. Both a photon beam and an ion beam are focused into the entrance volume of a cylindrical mirror analyzer. Also shown is the photoelectron signal at two different photon energies, one on a Ca^+ resonance, the other off the resonance. From Bizau *et al.*, Physical Review Letters **67**, 576 (1991). Measurements made at Super ACO.

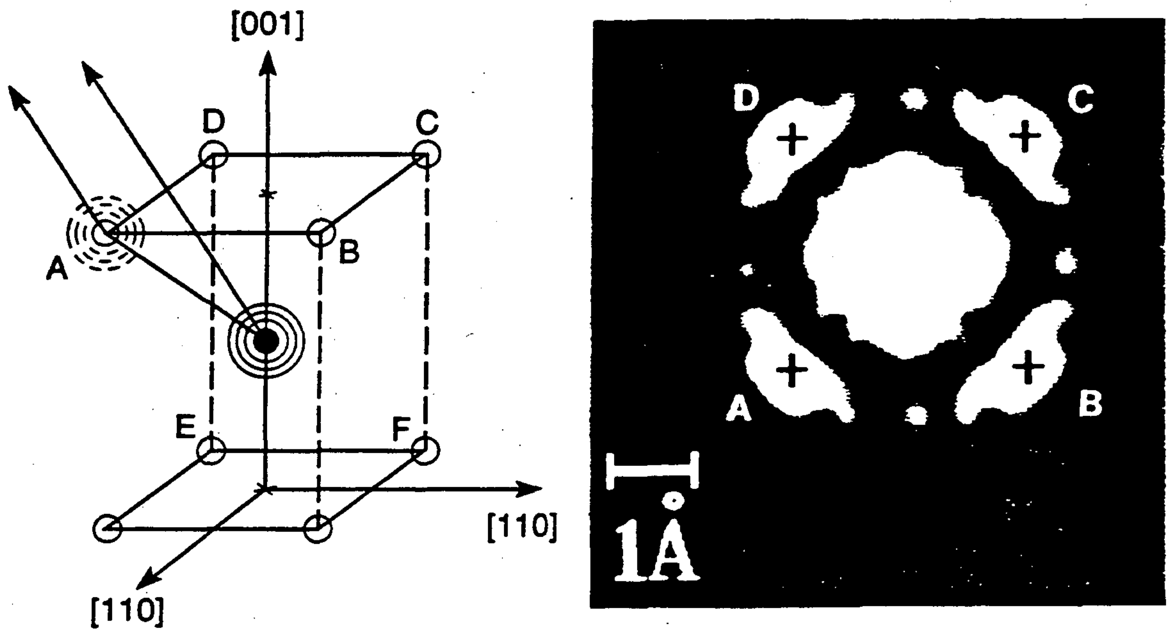

Figure 29. Holographic reconstruction of Cu(001). From Harp *et al.*, Physical Review Letters **65**, 1012 (1990); Physical Review B **42**, 9199 (1990).

5. Summary

A new generation of low-energy synchrotron storage rings will produce extremely bright beams of vacuum-ultraviolet and soft x-ray radiation. The high spatial and spectral resolution, along with polarization control, coherence, and a short-pulse time structure present new opportunities for research in a wide variety of fields, including atomic and molecular physics and chemistry, surface and materials sciences, biology and life sciences, and technology. This NATO Advanced Study Institute is devoted to exploring some of these opportunities.

Acknowledgements

My thanks to Gloria Lawler and Arthur Robinson for their kind assistance in writing this manuscript. This work was supported by the Director, Office of Energy Research, Office of Basic Energy Sciences, of the U.S. Department of Energy, under contract DE-AC03-76SF00098.

LAWRENCE BERKELEY LABORATORY
UNIVERSITY OF CALIFORNIA
TECHNICAL INFORMATION DEPARTMENT
BERKELEY, CALIFORNIA 94720